

Intracranial stent visualization for image guided interventions and therapy

Daniel Ruijters, Peter van de Haar, Ruben Roijers, Niels J. Noordhoek,
Jan Timmer, and Drazenko Babic

interventional X-Ray, Philips Healthcare, the Netherlands,
danny.ruijters@philips.com

Abstract. In intracranial interventional treatment there is currently an increased interest in applying stents with a very low X-ray radiopacity. These types of stents are nearly invisibility in standard 2D imaging. Flat Detector Computed Tomography (FDCT) CT offers a solution in imaging these stents peri-interventionally, and has become increasingly popular within minimally invasive endovascular interventions. Recent innovations in FDCT acquisition and 3D reconstruction techniques have considerably improved the feasibility to visualize stents that possess very little radiopacity. However, stents that are placed adjacent to aneurysms filled with coils lead to reconstructed images that are severely distorted by streaking artifacts, caused by the metal coils. In this article, results are presented regarding the FDCT acquisition and visualization of intracranial stents and the reduction of streaking artifacts in a second pass reconstruction.

1 Introduction

In recent years the imaging capabilities of flat-detector C-arm X-ray systems have been improved. These systems are essentially the eyes of the physician during stent navigation, placement and deployment. Technical developments such as Flat-Detector Computed Tomography (FDCT) for imaging of the vasculature and soft-tissue offer a previously unprecedented high quality visualization of anatomy and devices during interventional treatment [1, 2]. Also algorithmic developments, like metal artifact reduction techniques, have contributed to the advances with respect to intracranial stent visualization. These developments offer the possibility to inspect the stent deployment with respect to the vessel lumen and intravascular plaques. On the other hand, recent developments in stent technology have led to stents, e.g. Nitinol stents, which are increasingly difficult to visualize. In this article, we will discuss the technological advances with respect to intracranial stent placements and the associated challenges.

2 FDCT for soft-tissue imaging

Flat-detector cone-beam CT is primarily used to assess the soft-tissue structures during interventional treatment. The FDCT data is acquired using a neuroangiographic X-ray C-arm (Allura Xper FD20; Philips Healthcare, Best, the

Netherlands), equipped with a cesium iodide - amorphous silicon flat panel detector. The sensor area of the flat detector measures approximately 30 x 40 cm and consists of 1920 x 2480 pixels. The cone beam acquisition protocol consists of a rotational trajectory over a 200 arc while acquiring 620 projection images. The source-to-detector distance is 1195 mm. The objects of interest should be positioned in the center of rotation, 810 mm from the source. The X-ray tube voltage is set to 120 kV, the focal spot to 0.7 mm, and a copper filter of 0.4 mm is used. The associated radiation dose ranges from 45 to 49 mGy CTDI dose. Pre-processing steps of the projection images include gain correction, scatter correction, water beam-hardening correction, and Parker weighting [3]. The 3D reconstruction is obtained using the Feldkamp-Davis-Kress method [4]. Figure 1 presents a reconstruction of a Catphan phantom showing the contrast resolution for inserts of various sizes. As can be observed, 5 HU differences are still visible for larger inserts [5].

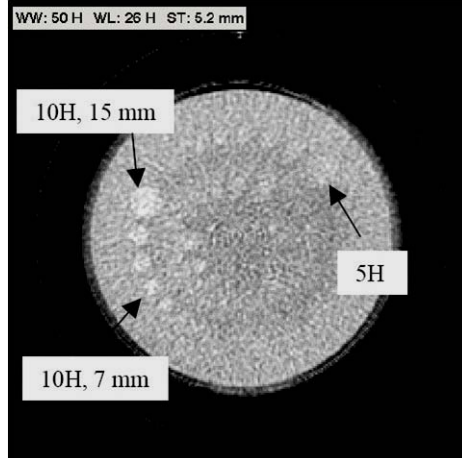


Fig. 1. XperCT reconstruction of a Catphan phantom with inserts of different contrast and sizes [5].

3 High resolution FDCT

While the previously described cone-beam CT protocol is very well suited for soft-tissue imaging, it is sub-optimal for stent imaging. For the purpose of imaging intracranial stents and their surrounding vasculature a dedicated acquisition protocol and reconstruction settings were developed (VasoCT; Philips Healthcare, Best, the Netherlands). The high resolution protocol also consists of 620 projection images, but the imaged detector area is fixed to a diameter of 22 cm with a pixel size of 0.154 mm, allowing very high spatial resolution 3D reconstructions. The X-ray tube voltage is set to 80 kV, the focal spot to 0.4 mm,

while no copper filter is being used. Figure 2 compares the soft-tissue and the high resolution protocols in a porcine in-vivo acquisition [3]. Figure 3 shows a stent acquired in an in-vitro setup, using the soft-tissue and the high resolution protocols [6]. The high resolution protocol can be combined with the injection of iodine contrast medium (either an intravenous injection, or an on-site intra-cranial injection of diluted contrast), in order to inspect the interface of the stent and vessel lumen. In this manner it is possible to assess whether the stent has been properly deployed.



Fig. 2. Left: standard XperCT acquisition of stents placed in a swine model, Right: high resolution acquisition of the same part. Adapted from Patel *et al.* [3].

4 Metal Artifact Reduction

In the first step of the Metal Artifact Reduction (MAR) algorithm [7] a regular filtered back-projection reconstruction is produced [4]. From this reconstruction the volumetric regions that display high X-ray absorption are isolated, using a predefined threshold. These regions are then forward projected [8] on the original X-ray images, in order to identify the high-absorption areas in the images. In the second pass, the identified areas in the original X-ray images are replaced by linearly interpolated grey-values from the surrounding scan lines (see Figure 4).

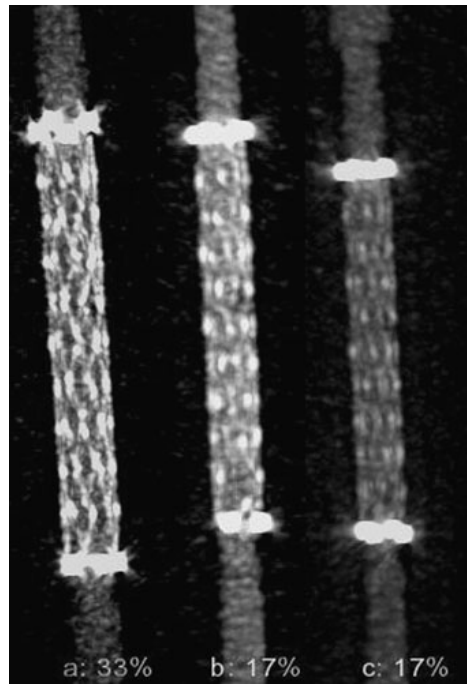


Fig. 3. A Wingspan nitinol stent. A comparison between a high-resolution/high-contrast case, b standard resolution/ high-contrast case, and c the standard resolution/standard contrast case. In all cases, an intra-tube high-density contrast agent of 550 HU was applied [6].



Fig. 4. The high-absorption areas in the rotational X-ray acquisition images (arrows: coils, teeth fillings) have been replaced by linear interpolation of their surrounding scan line values.

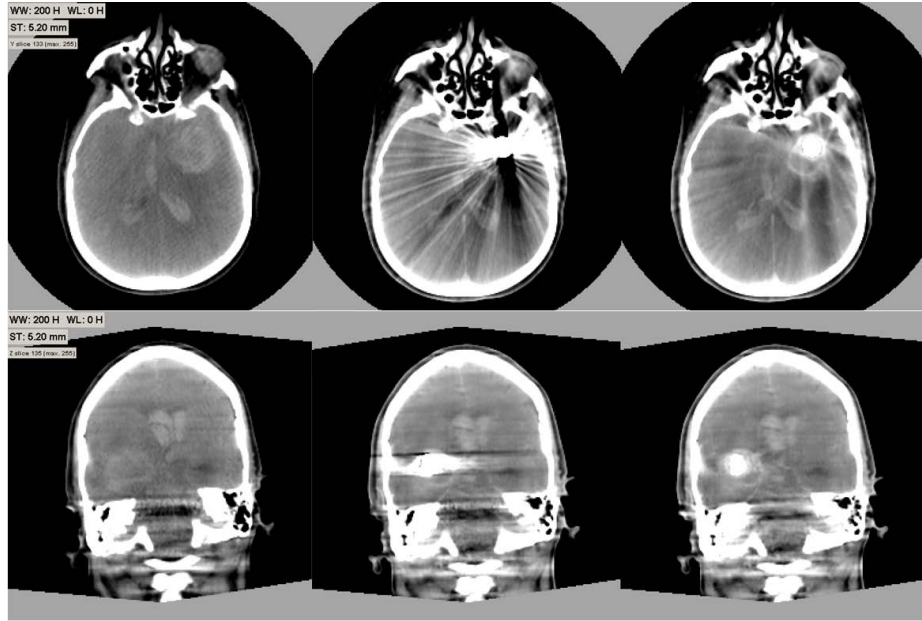


Fig. 5. Left images: reconstruction prior to coiling. Middle images: reconstruction post coiling, without MAR. Right images: same acquisition in the middle, but the reconstruction has been performed with MAR.

From these merged images a new filtered back projection reconstruction is calculated in the second pass. The entire process of two passes is performed within about 150 seconds.

The effect of the MAR technique is illustrated in Figure 5. From the same patient a FDCT acquisition was made prior and post coiling an aneurysm. The 3D reconstruction of the prior coiling acquisition obviously does not display any streaking artifacts. The post coiling reconstruction is severely distorted with streaking artifacts in the reconstruction without MAR. The post coiling reconstruction with MAR clearly suffers far less from streaking artifacts.

The MAR procedure significantly reduces the presence of metal streaking artifacts caused by coils placed in aneurysms. This allows the investigation of the tissues and anatomical structures adjacent to the coiled volume. In case of stent/coils combinations this is especially valuable, since the streaks tend to obscure the intracranial stent in the reconstruction plane.

MAR cannot fully remove all metal artifacts. Typically, some streak-artifacts remain. The intensity of the remaining streaks depends on complexity of nearby anatomy (like bone structures), size of metal object etc. Soft-tissue imaging of very low-contrasts will still suffer from artifacts, but the artifact level is significantly reduced. Overall the diagnostic value of the MAR reconstructed images is greatly enhanced.

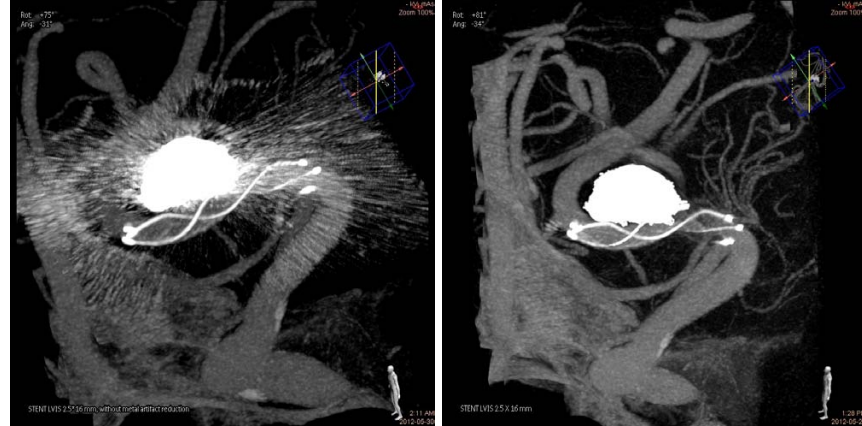


Fig. 6. High resolution reconstruction with coiled aneurysm and stent. Left: without metal artifact reduction, Right: with metal artifact reduction applied.

Particularly, when diluted iodine contrast medium has been administrated, enabling the examination of the vascular morphology, the streaking artifacts severely disturb the evaluation of the aneurysm neck. Furthermore, false vessel bifurcations and branches may be introduced by the streaking artifacts. The MAR procedure largely resolves these disturbing phenomena. It removes the false bifurcations and branches, and enables the clear visualization of the aneurysm neck, see Figure 6. The high resolution reconstruction also allows assessing the stent placement and deployment with respect to the vessel lumen.

5 Conclusions

Several technical advancements have been presented with respect to intracranial stent imaging during minimally invasive image guided interventional treatment. Flat Detector cone-beam CT enables to assess the soft-tissue structures in a peri-interventional setting. Though the contrast resolution up to 5 HU is already acceptable for many applications, it is still not good enough to detect fresh small hemorrhages, although larger bleedings can be observed.

The high resolution protocol enables an unprecedented high spatial 3D resolution for assessment of intracranial stent deployment. Vessel lumen, plaque, and intravascular devices are clearly visualized with well defined interfaces with as result better outcome control leading to a more successful endovascular treatment.

The employment of metal artifact reduction in coiled aneurysms combined with stent placement significantly increases the accuracy of the procedure, since it enables, for the first time, a correct assessment of stent location and deployment in the catheterization laboratory.

Especially, the combination of the high resolution acquisition protocol together with metal artifact reduction proves to be valuable during minimally invasive endovascular intracranial stent placement for stents that are placed adjacent to coiled aneurysms (as can be seen in Figure 6), since the high resolution protocol enables the visualization of the very fine stent struts, while the metal artifact reduction considerably reduces the streaking artifacts which otherwise may hamper the inspection of the deployment of the stent.

References

1. Söderman, M., Babic, D., Holmin, S., Andersson T: Brain imaging with a flat detector C-arm, Technique and clinical interest of XperCT. *Neuroradiol* 50:863-868 (2008)
2. Kamran, M., Nagaraja, S., Byrne, J.V.: C-arm flat detector computed tomography: the technique and its applications in interventional neuro-radiology. *Neuroradiol* 52:319-27 (2010)
3. Patel, N.V., Gounis, M.J., Wakhloo, A.K., Noordhoek, N., Blijd, J., Babic, D., Takhtani, D., Lee, S.-K., Norbash, A.: Contrast-Enhanced Angiographic Cone-beam CT of Cerebrovascular Stents: Experimental Optimization and Clinical Application. *AJNR* 32:137-144 (2011)
4. Feldkamp, L.A., Davis, L.C., Kress, J.W.: Practical cone-beam algorithm. *J Opt Soc Am A* 1:612-19 (1984)
5. Noordhoek, N.J., van de Haar, P.G., Timmer, J.: Direct comparison of commercially available C-arm CT to multislice CT image quality. *Proc. RSNA*, Chicago, USA (2006)
6. Snoeren, R.M., Söderman, M., Kroon, J.N., Roijers, R.B., de With, P.H.N., Babic, D.: High-resolution 3D X-ray imaging of intracranial nitinol stents. *Neuroradiology* 54(2):155-162 (2012)
7. Prell, D., Kyriakou, Y., Struffert, T., Dorfler, A., Kalender, W.A.: Metal Artifact Reduction for Clipping and Coiling in Interventional C-Arm CT. *AJNR Am J Neuroradiol* 31:634-39 (2010)
8. Ruijters, D., ter Haar Romeny, B.M., Suetens, P.: GPU-Accelerated Digitally Reconstructed Radiographs. *Proc. IASTED BioMed*:431-435 (2008)